Integrated Design and Optimization of Microelectronic Devices

Tom Cwik and Gerhard Klimeck
Jet Propulsion Laboratory
California Institute of Technology
4800 Oak Grove Dr.
Pasadena Ca, 91109
818-354-4386
cwik@jpl.nasa.gov

Abstract—A genetic algorithm is used for design of infrared filters and in the understanding of the material structure of a resonant tunneling diode. These two components are examples of microdevices and nanodevices that can be numerically simulated using fundamental mathematical and physical models. Because the number of parameters that can be used in the design of one of these devices is large, and because experimental exploration of the design space is unfeasible, reliable software models integrated with global optimization methods are examined. The genetic algorithm and engineering design codes have been implements on massively parallel computers to exploit their high performance. Design results are presented for the infrared filter and a resonant tunneling diode.

TABLE OF CONTENTS

1. INTRODUCTION

The NASA/JPL goal to reduce payload in future space missions while increasing mission capability demands miniaturization of active and passive sensors, analytical instruments and communication systems among others. Currently, typical system requirements include the detection of particular spectral lines, associated data processing, and communication of the acquired data to other systems. Advances in lithography and deposition methods result in more advanced devices for space application, while the sub-micron resolution currently available opens a vast design space. Though an experimental exploration of this widening design space—searching for optimized performance by repeated fabrication efforts—is unfeasible, it does motivate the development of reliable software design tools. These tools necessitate models based on fundamental physics and mathematics of the device to accurately model effects such as diffraction and scattering in opto-electronic devices, or bandstructure and scattering in heterostructure devices. The software tools must have convenient turn-around times and interfaces that allow effective usage. The first issue is addressed by the application of high-performance computers and the second by the development of graphical user interfaces driven by properly developed data structures. These tools can then be integrated into an optimization environment, and with the available memory capacity and computational speed of high performance parallel platforms, simulation of optimized components can proceed. In this paper, specific applications of the electromagnetic modeling of light coupling and filtering, as well as heterostructure device design will be presented.

The first application involves detectors and filters of long-wavelength infrared radiation that are under development for a wide range of applications. Over this band (3-18 μm) applications range from spaceborne sensors used in the examination of absorption spectra to ground based hand-held digital cameras. Electromagnetic fields that interact with active quantum well layers or are filtered by periodic structures are modeled by Maxwell's equations and discretized by finite element methods. An integrated design involves CAD generation of the microdevice structure, generation of a mesh that will discretize the fields, an accurate solution of the electromagnetic fields, and visualization of the resultant field solution. This suite of tools is then integrated into a parallelized genetic algorithm package for design optimization.

The second application involves the heterostructure device design and involves the choice of material composition, layer thicknesses and doping profiles. A general-purpose quantum-mechanics based one-dimensional design and analysis tool is used for modeling. As in the above application, this tool is integrated with the parallelized genetic algorithm package for design optimization.

2. OPTIMIZATION VIA GENETIC ALGORITHMS

Due to the number of parameters involved in instrument design and the broad classes of design optimization needed, global optimization algorithms are considered. A key consideration in using global methods is that they optimize over a carefully defined set of parameters where each parameter is confined to a limited range. Though local optimization methods can be employed, they have been found to be highly dependent on starting points, and are typically more successful when the solution space is a

relatively smoothly varying function of the design parameters. In the device models considered in this paper, the solution space is non-linear and can appear to be nearly a discontinuous function of the design parameters over regions of the design space. The local methods deploying gradient searches are then difficult to employ for such multi-parameter optimization.

Genetic algorithm optimization employs stochastic methods modeled on principles of natural selection and evolution of biological systems [1,2]. They are global, multi-parameter and do not require constraints on continuity of the solution space. They have been introduced in electromagnetic design and modeling over the last 5 years [3-6] in the relatively diverse areas of antenna design, filter design and the design of scattering structures. The work in electronic structure modeling and optimization is more recent [7-9]. At JPL an effort is underway to advance the capabilities for electromagnetic and electronic structure modeling of select microdevice structures. A genetic algorithm package that is easy and flexible to use is part of this effort.

A genetic algorithm optimization package consists of a sequence of procedures that lead to an optimized result. This sequence is common among all genetic algorithms with variants at each stage [2]:

1. Model parameterization and gene encoding.
2. Initialization of population.
3. Evaluation of fitness function for population.
4. Selection of subset of population.
5. Reproduction through crossover and mutation.
6. Evaluation of fitness function and convergence check.

This process is diagrammed in Figure 1 and is the basis for a general package. Because each step in this sequence would require variants dependent on the problem being optimized, a long-term goal is to provide a software framework that is suitable for the select class of design

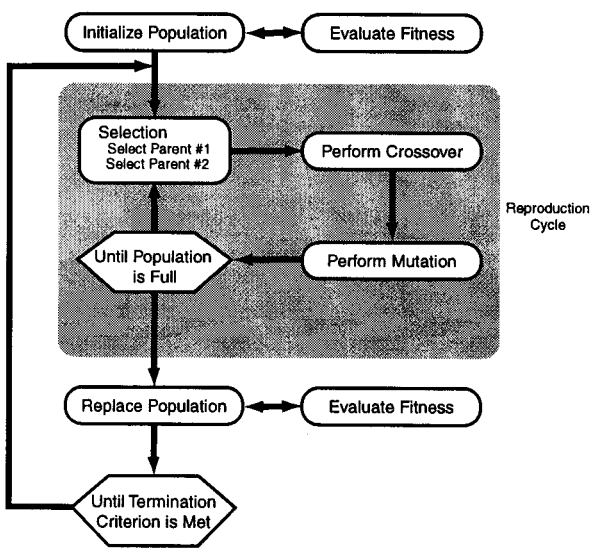

Figure 1 Genetic Algorithm flow diagram. (From [5].)

problems considered in this paper. For example, an interface into the range and types of parameters encountered (real-valued device dimension values, integer valued number of layers, or exponent based dopant densities) is to be developed. Similarly an effective means for introducing the fitness function evaluation, i.e. the actual calculation of the electromagnetic or electronic structure result is necessary. This step requires the insertion of large complex codes, typically written in C or Fortran with associated complex input sets, into the software framework. Ideally there would be little modification of the solver codes when using the genetic algorithm package.

One of the most important stages of the optimization process is the sound parameterization of the design and resultant encoding of the parameterization into a chromosome. The parameters need to be chosen from the design space in an effective manner, limited in range to a set that is physical, and encoded in a meaningful way. For example, the critical device dimensions are typically used, as well as the device material values. If a grid based algorithm such as a finite element solver is used the geometry must be properly parameterized at the CAD stage before a mesh is generated. The geometry should vary in meaningful steps such that known electromagnetic or electronic properties will vary a non-vanishing amount. This variation of geometry or material parameters maps into the stages of population initialization and reproduction through mutation. By allowing variations in the dimensions or materials that produce physically different results, fewer genes need to be stochastically sampled and convergence to an optimum result can occur quicker. Similarly, how the parameter is encoded into a gene is important. For example encoding a real parameter into a binary string or using real-valued encoding is itself a tradeoff [6]. In general, efficient convergence of the optimization algorithm will heavily depend upon the initial parameterization and encoding of the design.

A number of genetic algorithms and packages exist that fit the structure outlined in Figure 1. The key needs for the work in this paper are that the package be flexible enough to allow a range of design parameterizations and be able to exploit high performance computers. First, the different parameterizations and encodings, as well as mutation strategies need to be easily available. Secondly, because the calculations of the fitness function involve electromagnetic and electronic structure calculations that can be quite intensive, executing the genetic algorithm on massively parallel computers is essential for high-fidelity models. These points are encapsulated in PGAPack, a parallel genetic algorithm library [10]. This package consists of a set of library routines supplying the user multiple levels of control over the optimization process. The levels vary from default encodings, with simple initialization of parameters and single statement execution, to the ability to modify, at a low-level, all relevant parameters in the optimization process. User written routines for evaluation or crossover and mutation can also be inserted if necessary. The package is written using the Message Passing Interface (MPI) for parallel execution on a number of processors. A master process coordinates the chromosome initialization, selection

and reproduction while slave processes calculate the fitness function, including the execution of the electromagnetic or electronic structure code on different processors. For global optimization of realistic structures, the use of high-performance computers is essential to allow designs in a reasonable amount of time. The bottleneck of the optimization process is the electromagnetic or electronic structure code calculation. This result is then used in a calculation of a fitness function (the difference between the calculated and desired result) that is minimized. It is also important that the engineering code be optimized to speed the overall time to design.

3. Electromagnetic Modeling of Infrared Filters

Two electromagnetic modeling applications are currently being considered for optimization. The first involves design of multi-bandwidth infrared filters for multi-spectral imagers. The second involves the design of light coupling structures for quantum well infrared photodetectors and uses finite element modeling of Maxwell's equations. This application will not be considered in this paper; the filtering application will be given in detail.

Multi-Spectral Filtering

A multi-bandwidth infrared filter array consists of an array element within a two-dimensional periodic cell. The filter bandwidth, center frequency and polarization properties are dependent upon the shape and size of this element. Different element shapes are used for different applications depending on the design specification. To model a single layer frequency selective surface, a calculation for the induced current on the metallic periodic array deposited on a layered substrate is performed. To model the multiple layering of the design, the scattering parameters due to each screen are cascaded in a separate calculation. The frequency selective surface analysis uses sub-domain basis functions to model the current in a periodic cell. An overview of the analysis is now developed [11].

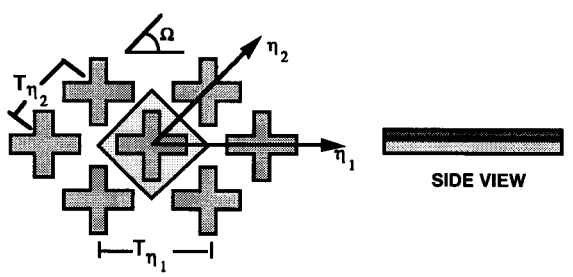

Figure 2. Geometry of crossed-slot frequency selective surface. Plan view and side views are shown.

Single Layer Frequency Selective Surface Analysis

The geometry of a crossed slot periodic surface is shown in Fig. 2. Periodicities are T_{η_1} and T_{η_2} in the non-orthogonal (η_1, η_2) coordinate system. Multiple dielectric layers are included below and above the metal slot array. The scattered electric field in all space due to an induced current may be found from the source-field relationship

$$\bar{E}^s(\bar{\rho},z) = \frac{1}{j\omega\varepsilon}(\nabla\nabla + k^2\mathbf{I})\cdot\bar{A}(\bar{\rho},z) \tag{1}$$

where the vector potential is

$$\bar{A}(\bar{\rho},z) = \int_{-\infty}^{+\infty}\bar{J}(\bar{\rho}',z)\frac{e^{-jkR}}{4\pi R}d\bar{\rho}' \tag{2}$$

and the distance R is $[(x-x')^2+(y-y')^2+z^2]^{1/2}$ (The current lies in the plane z' = 0 without loss of generality.) Consistent with Floquet's condition, the support of the current may be reduced from that existing over the entire plane z' = 0 to that of one cell, i.e.,

$$\bar{J}(\bar{\rho}) = \sum_{mn=-\infty}^{\infty}\tilde{\bar{J}}_{mn}\Psi_{mn}(\bar{\rho}) \tag{3a}$$

where

$$\tilde{\bar{J}}_{mn} = \int_{\partial S}\bar{J}(\bar{\rho}')\Psi^*_{mn}(\rho')d\bar{\rho}' \tag{3b}$$

and where the transverse component of the m,nth Floquet harmonic is

$$\Psi_{mn}(\bar{\rho}) = \frac{1}{(T_xT_y)^{1/2}}e^{j\bar{k}_{mn}\cdot\bar{\rho}} \tag{4}$$

The associated propagation constant is

$$\bar{k}_{mn} = \hat{x}k_{x_m} + \hat{y}k_{y_n} \tag{5}$$

where

$$k_{x_m} = \frac{2\pi}{T_x}m + k_{x_0} \tag{6a}$$

$$k_{y_n} = \frac{2\pi}{T_y}n + k_{y_0} \tag{6b}$$

The z component of the propagation vector is

$$k_{z_{mn}} = (k^2 - k_{x_m}^2 - k_{y_n}^2)^{1/2} \tag{7}$$

and the negative imaginary branch is taken when $k_{x_m}^2 + k_{y_n}^2 > k^2$.

Equation (3) defines a transform pair and is recognized as the Fourier series representation of the induced current multiplied by the phase of the incident field. A direct construction of the scattered field in terms of the Floquet harmonics involves the transform of the free-space Green's function.

$$\frac{e^{-jkR}}{4\pi R} = \frac{1}{(2\pi)^2}\int_{-\infty}^{\infty} \frac{e^{-jk_z|z|}}{2jk_z} e^{j\bar{k}\cdot(\bar{\rho}-\bar{\rho}')}\, d\bar{k} \qquad (8)$$

where the propagation vector is continuous. Substituting the Floquet representation of the current (3a) along with the Fourier representation of the Green's function into the potential results in

$$\bar{A}(\rho,z) = \sum_{mn=-\infty}^{\infty} \tilde{\bar{J}}_{mn} \frac{e^{-jk_{z_{mn}}|z|}}{2jk_{z_{mn}}} \Psi_{mn}(\bar{\rho}) \qquad (9)$$

Summations and integrations have been interchanged, and use has been made of the transform pair

$$\frac{1}{(2\pi)^2}\int_{-\infty}^{\infty} e^{j(\bar{k}_{mn}-\bar{k})\cdot\bar{\rho}}\, d\bar{\rho} = \delta(\bar{k}_{mn}-\bar{k}) \qquad (10)$$

Completing the indicated differentiations of (1) results in the representation of the scattered electric field

$$\bar{E}^s(\rho,z) = \frac{1}{j\omega\varepsilon}\sum_{mn}\frac{1}{2jk_{z_{mn}}}\begin{bmatrix} k^2-k_{x_m}^2 & -k_{x_m}k_{y_n} \\ -k_{x_m}k_{y_n} & k^2-k_{y_n}^2 \end{bmatrix}\cdot \tilde{\bar{J}}_{mn}\Psi_{mn}(\bar{\rho})e^{-jk_{z_{mn}}|z|}$$

$$= \frac{1}{j\omega\varepsilon}\sum_{mn} Z_{mn}\cdot\tilde{\bar{J}}_{mn}\Psi_{mn}(\bar{\rho})e^{-jk_{z_{mn}}|z|} \qquad (11)$$

The scattered magnetic field may be similarly found from the relation

$$\bar{H}^s(\bar{\rho},z) = \nabla\times\bar{A}(\bar{\rho},z) \qquad (12)$$

The Impedance Boundary Condition

To account for losses in the metallic material, an impedance boundary condition is used. A rigorous examination of non-perfectly conducting surfaces would require the calculation of induced volume currents in the lossy material. (The metallic region would have an electrical thickness dependent upon material parameters and wavelength.) The surface impedance boundary condition allows the volume formulation to be approximated by an analysis considering only the surface current and is written as

$$\bar{E}^i + \bar{E}^s = R\bar{J} \qquad (13)$$

where tangential fields are implied and the equation holds over the support of the current. The complex impedance R depends upon the material parameters and electrical thickness of the metal. For metallic materials which greatly attenuate the field as it penetrates the medium, R is the medium impedance $\sqrt{\mu/\varepsilon}$ where ε is the complex permittivity of the medium. Conversely, for materials which allow little attenuation and phase shift of the field as it penetrates the medium, R is $\sqrt{\mu/\varepsilon}/kt$ where k is the complex propagation constant of the material and t is the thickness of the patch. With the scattered field given by (11), the impedance boundary condition is written as

$$R\bar{J} - \frac{1}{j\omega\varepsilon}\sum_{mn} Z_{mn}\cdot\tilde{\bar{J}}_{mn}\Psi_{mn} = \bar{E}^i \qquad (14)$$

where tangential components in the z = 0 plane are implied. For materials in the infrared, measurements give the loss factors for metals used, and indicate that the first approximation above is to be applied. This approximation can be improved by using volumetric techniques such as a finite element method to calculate fields in the lossy materials.

Sub-Domain Expansion Functions

Equation (14) is the unique relation for the induced current with its solution yielding the reflection and transmission coefficients of the structure. To model an arbitrary size crossed-slot or other shape within the periodic cell, sub-domain rooftop basis functions are chosen to represent the current. This is especially important in patterned arrays that do not conform to standard shapes as in microwave design. These functions model the current distribution and allow the scattered field to be given by a convergent series. As seen in Fig. 3, the normal component of current approaches zero at the patch edges, and is nonzero when tangential to the edges, allowing for the representation of the edge singularity. Each subsection of current extends over two patches of the grid, longer in the direction of the current, with at least one x-directed and y-directed rooftop overlaying each patch. The subsection is sampled at the center of each rooftop.

As shown in Fig. 3, the sample points of each subsection of

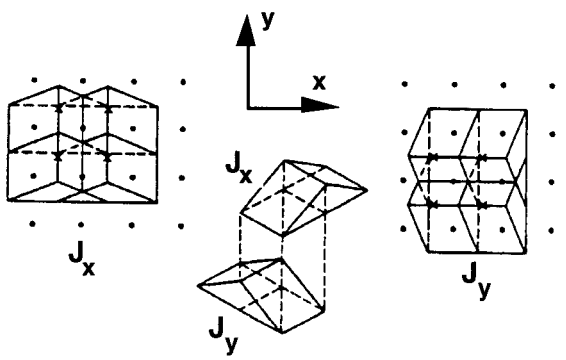

Figure 3. Diagram of rooftop sub-domain basis functions used to represent current.

current are shifted from the center point of its associated patch. A coordinate system is chosen such that the sample points of the grid lie at the center of each patch. The sample points of the rooftops representing the y-component of the current are then shifted to the edge of the patch in the positive x direction, and similarly, the sample points of the rooftop representing the y-component of the current are shifted to the edge of the patch in the positive y direction.

Cascade Connection of Scattering Parameters

The dominant mode reflection and transmission coefficients are found from the induced current

$$R_0 = \frac{-\omega\mu}{4E_0}\frac{1}{2jk_{z_0}}\tilde{J}_0 \tag{15a}$$

$$T_0 = 1 - \frac{\omega\mu}{4E_0}\frac{1}{2jk_{z_0}}\tilde{J}_0 \tag{15b}$$

To model the multiple layers of the frequency selective surface, scattering parameters of each single frequency selective surface layer are calculated and cascaded [12]. The scattering parameters include the dominant harmonic coefficients in (15) and higher-order harmonics. The single layer frequency selective surface consists of the metallic array and any number of other dielectric layers that may exist. The scattering parameters for this sandwich structure are calculated and then combined with those of other layers of possible different element sizes. A composite scattering matrix

$$\begin{bmatrix} \overline{V}^{\alpha_s} \\ \overline{V}^{\gamma_s} \end{bmatrix} = \begin{bmatrix} \mathbf{S}^{\Sigma}_{\alpha\alpha} & \mathbf{S}^{\Sigma}_{\alpha\gamma} \\ \mathbf{S}^{\Sigma}_{\gamma\alpha} & \mathbf{S}^{\Sigma}_{\gamma\gamma} \end{bmatrix} \cdot \begin{bmatrix} \overline{V}^{\alpha_i} \\ \overline{V}^{\gamma_i} \end{bmatrix} \tag{16}$$

is computed which contains the transmission and reflection coefficients of the entire frequency selective surface.

Parameterization and Results

For the multi-spectral imager application, the goal is to create a filter with a prescribed center wavelength and bandwidth of the transmission response. The filter consists of patterned metal layers fabricated using electron beam lithography. An array of apertures is patterned into a gold layer deposited on a calcium fluoride substrate. The key parameters of the design are the element shape, periodicities in the x and y direction as well as the skew angle Ω, thicknesses of dielectric superstrate and substrate layers, and distance between layers of a sandwich structure.

The fitness function for this application is driven by the requirement of a prescribed center wavelength and bandpass with minimal shoulders outside the bandpass region. A typical response with parameters is shown in Figure 4. The center wavelength, as well as upper and lower edges of the passband is specified. The fitness function specified for this application is a weighted combination of the prescribed center wavelength and a measure of the energy outside the

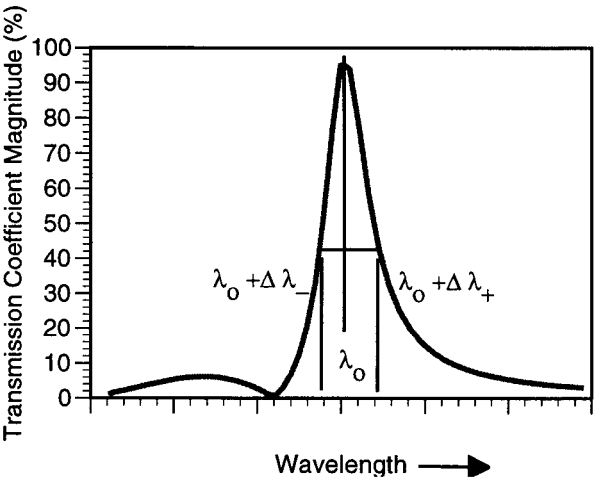

Figure 4. Fitness function design for filter example. Center wavelength and lower and upper bounds of bandpass region are noted.

center band. This component is calculated by dividing the area under the square of the transmission curve outside the center band by the total area squared under the transmission response. The goal in this specification is to reduce any energy outside the bandpass region for an optimal multi-band filter design.

The code for the analysis of the frequency selective screen was integrated with PGAPACK and executed on a 256 CPU HP Exemplar X-Class massively parallel processor. For an initial design the center wavelength was chosen to be 4 micrometers, and the bandwidth was minimized outside a region with a 5% (full) bandwidth. A one millimeter thick calcium floride substrate (n = 1.41) was included in the calculation as well as the surface impedance of gold in the near-infrared. A previous design, created without the use of the genetic algorithm optimization package, was used as a 'strawman' to be equaled or bettered. Optimization was carried out using the cell size as a parameter and fixing the element geometry to a crossed dipole aperture. Shown in Figure 5 is the resultant design as well as a set of measurements of the fabricated model [13]. For this limited set of optimization parameters, the previous design was equaled but not bettered. The design simulation though was completed with one execution of the genetic algorithm, exhausting the limited set of global parameters needed to minimize the fitness function outlined above. Additional designs with an expanded parameter space are under consideration.

4. Electronic Structure Calculations

The electronic structure calculations considered in this section involve heterostructure device designs being considered at the Jet Propulsion Laboratory. While silicon device technology dominates the commercial microprocessor

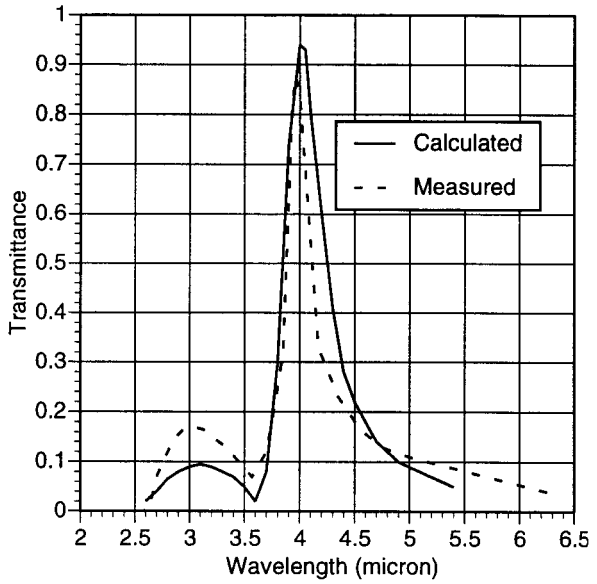

Figure 5. Comparison of numerical simulation and measured transmission spectra for infrared filter.

and memory market, semiconductor heterostructure devices maintain their niche for light detection, light emission, and high-speed data transmission. The production of these heterostructure devices is enabled by the advancement of material growth techniques that have opened up a vast design space. The full experimental exploration of this design space is unfeasible and a reliable design tool is needed.

Military applications have similar system requirements to those listed above. Such requirements prompted a device modeling project at the Central Research Laboratory of Texas Instruments (which transferred to Raytheon Systems in 1997). The Nanoelectronic Modeling Tool (NEMO) was developed as a general-purpose quantum mechanics-based one-dimensional device design and analysis tool from 1993-97. The tool is available to US researchers by request on the NEMO web site [14]. NEMO is based on the non-equilibrium Green's function approach, which allows a fundamentally sound inclusion of the required physics: bandstructure, scattering, and charge self-consistency. The theoretical approach is documented in references [15, 16] while some of the major simulation results are documented in references [17-19].

Heterostructure device designs involve the choice of material compositions, layer thicknesses, and doping profiles. Material parameters such as band offsets, effective masses, dielectric constants etc. influence the device simulation results in addition to the structural design parameters. The full exploration of the design space using purely experimental techniques is unfeasible due to time and financial constraints. For example, it takes a well-equipped research laboratory approximately five working days [20] for the growth, processing and testing of a particular resonant tunneling diode design. NEMO can provide quantitative [17-19] current voltage characteristics (I-V's) within minutes to hours [20] of CPU time for a single set of device and material parameters. With this quantitative simulation capability the design parameter space can be explored expediently once an automated system for the design parameter variation is implemented. As in the electromagnetic filtering application considered in Section 3 a fitness function is developed, and the NEMO code is integrated into the optimization framework of Figure 1, interfacing to PGAPACK.

Simulation Target and Fitness Function

In this work the resonant tunneling diode is used as a vehicle to study the effects of structural and doping variations on the electron transport. The structure of the device consists of a number of monolayers, with associated doping levels. Current-voltage characteristics of two devices that are part of a well-behaved test matrix of experimental data published in reference [18] are used as a design target

The fitness of the simulated data is measured against a target current-voltage characteristic. There are four particular features that are explicitly evaluated for each simulated characteristic: peak and valley current and voltage, and the slope close to the peak and the valley (Figure 6). Differences between the target and the simulation in these four features and the absolute and relative error for all simulated data points enter into the fitness function with a weighted average. The target fitness evaluated against itself results in a value of 1. Disagreements between simulation and target result in fitness values between 0 and 1.

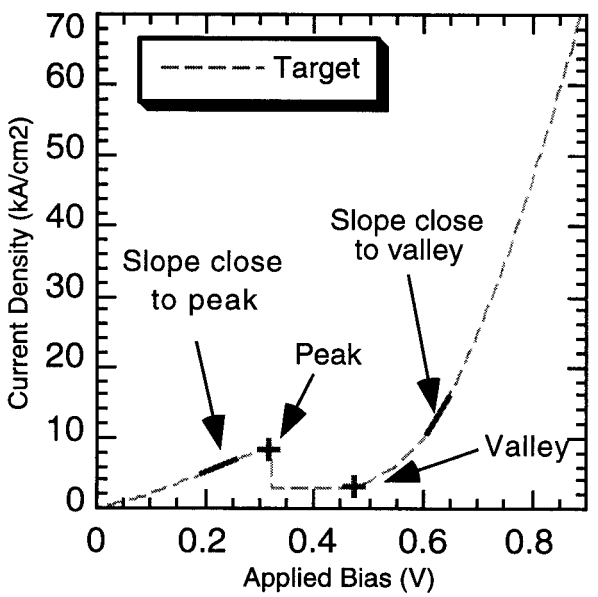

Figure 6. Features that enter into the evaluation of the fitness of simulated data. Of particular interest are the peak and valley voltage and current and the slopes close to the peak and the valley.

Results

In this numerical experiment, five parameters (2 doping concentrations, N_1, N_2, and 3 thicknesses, T_1, T_2, T_3) are

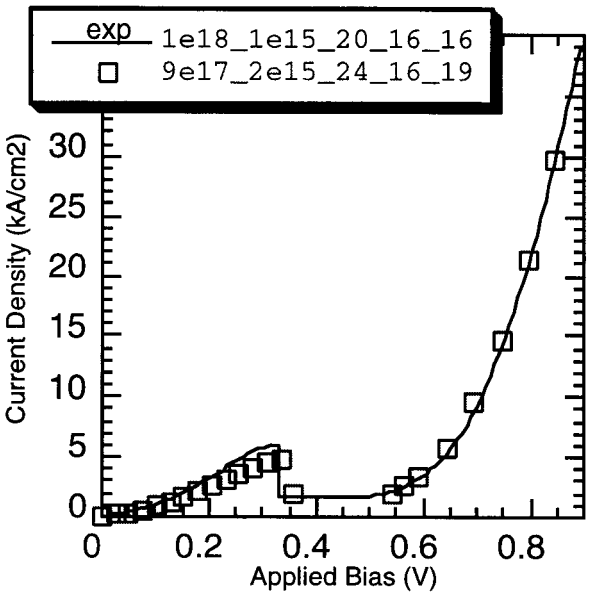

Figure 7: Current voltage characteristics of a InGaAs/InAlAs resonant tunneling diode. The nominal structures have barrier and well thicknesses of 16 monolayers (ml), and doping a doping profile of 10^{18} cm^{-3} (N_1) and 10^{15} cm^{-3} (N_2). The solid lines show experimental data published in reference [18], where the noise in the valley current region was eliminated. The curves are labeled by the 5 parameters `N1_N2_T1_T2_T3`.

varied within the genetic algorithm in order to achieve the best fit to an experimental I-V curve. The NEMO code is used to model the structure. This structure was specified to the grower to have 16 monolayers (ml) of barriers (T_2) and well (T_3), no intentional doping in the central device (N_2=1x10^{15} cm^{-3}), N_1=1x10^{18} cm^{-3} doping in the low doping spacers, and 3x10^{18} cm^{-3} in the high doping contacts. The no-doping spacer length T_1 is 20 ml. Further details of the structure can be found in [9]. The simulation is started from the random populations. The genetic algorithm converges to the nominal structure value, well within the experimental uncertainty as shown in Figure 7. Again it is found that the well widths must be increased in the simulation by a few monolayers versus the nominal values to achieve the best agreement with experimental data [18].

5. Conclusions

This paper has examined the use of a genetic algorithm for design of an infrared filter and for electronic structure modeling. A versatile genetic algorithm, PGAPACK, has been used for initial designs, optimizing realistic devices over broad design spaces. The optimization package has been integrated with the engineering simulation codes, and executed on parallel computational platforms. These advanced computational resources are necessary if advanced modeling codes are to be used to give high-fidelity simulations of micro-devices in the optimization process. Several wall-clock hours on the 64 CPU Exemplar were necessary to achieve the infrared filter design. The proper choice of parameters and proper encoding of these parameters into a chromosome used in the genetic algorithm is also necessary to efficiently reach an optimized solution.

Acknowledgements

The work described in this publication was carried out by the Jet Propulsion Laboratory, California Institute of Technology under a contract with the National Aeronautics and Space Administration. The supercomputer used in this investigation was provided by funding from the NASA Offices of Earth Science, Aeronautics, and Space Science. Part of the research reported here was performed using HP SPP-2000 operated by the Center for Advanced Computing Research at Caltech; access to this facility was provided by Caltech.

References

[1] J. Holland, *Adaptation in Natural and Artificial Systems*, Ann Arbor, The University of Michigan Press, 1975.

[2] D. Goldberg, *Genetic Algorithms in Search, Optimization and Machine Learning*, New York, Addison-Wesley, 1989.

[3] E. Michielssen, S. Ranjithan and R. Mittra, *Optimal Multilayer Filter Design Using Real Coded Genetic Algorithms,* Proc. Inst. Elect. Eng., pt. J, vol 139, no.12, pp. 413-420, 1992.

[4] R. Haupt, *Thinned Arrays Using Genetic Algorithms,*" IEEE Trans. Antennas Propag, AP-42, 7, pp. 939-999, July 1994.

[5] J. Johnson, and Y. Rahmat-Samii, *Genetic Algorithms in Engineering Electromagnetics*, IEEE Antennas and Propagation Magazine, Vol 939, No. 4, pp. 7-21, August 1997.

[6] C. Zuffada, and T. Cwik, "*Synthesis of Novel All-Dielectric grating Filters Using Genetic Algorithms*," IEEE Trans. Antennas Propag., Vol. 46, No. 5, pp.657-663, May. 1998.

[7] F. Starrost, S. Bornholdt, C. Solterbeck, and W. Schattke, *Band-Structure Parameters By Genetic Algorithm,* Physical Review B Condensed Matter, vol. 53, no. 19, pp. 12549-12552, May, 1996

[8] J. Krause, D. Reitze, G. Sanders, A. Kuznetsov, and C. Stanton, *Quantum Control In Quantum-Wells*, Physical Review B Condensed Matter, vol 57, no. 15, pp. 9024-9034, April 1998.

[9] G. Klimeck, C. Salazar-Lazaro, A., and T. Cwik, *Genetically Engineered Nanostructure Devices,* to be published in the Proceedings of the Material Research Society 1998.

[10] G. Levine, *Users Guide to the PGAPACK Parallel Genetic Algorithm Library,* Argonne Nat. Lab., 95/18, 1996.

[11] T. Cwik T. and R. Mittra., *Scattering from a periodic array of free-standing arbitrarily shaped perfectly conducting or resistive patches*, IEEE Trans. Antennas Propag., vol. AP-35, no. 11, pp. 1226-1233, Nov. 1987.

[12] T. Cwik T. and R. Mittra, *The cascade connection of planar periodic surfaces and lossy dielectric layers to form an arbitrary periodic screen*, IEEE Trans. Antennas Propag., vol. AP-35, no. 12, pp. 1397–1405, Dec. 1987.

[13] 4. Ksendzov, A., Fernandez, S., Cwik, T., La Baw, C. Maker, P. and Muller R., "*Wedge Filters for Spectral Imaging in the Near IR Using Metal Grids*, Proceedings Infrared Astronomical Instrumentation. Vol 3354 , 1998.

[14] NEMO, Nanoelectronic Modeling, in http://www.raytheon.com/rtis/nemo/.

[15] R. Lake, G. Klimeck, R. Bowen, D. Jovanovic, *Single And Multiband Modeling Of Quantum Electron-Transport Through Layered Semiconductor-Devices,* J-Appl-Phys v81 no. 12, pp7845-7869, June 1997.

[16] R. Lake, G. Klimeck, R. Bowen, D. Jovanovic, D. Blanks, et al., *Quantum Transport With Band-Structure And Schottky Contacts*, physica status solidi B, vol. 204 no. 1, pp 354-357, Nov. 1997.

[17] G. Klimeck, R. Lake, R. Bowen, W. Frensley, T. Moise, *Quantum Device Simulation With A Generalized Tunneling Formula*, Appl-Phys-L vol. 67, no. 17, pp. 2539-2541, Oct. 1995.

[18] G. Klimeck et al., *Quantitative Simulation of Strained and Unstrained InP-Based Resonant Tunneling Didodes,* IEEE DRC, 1997: p. 92.

[19] R. Bowen, G. Klimeck, R. Lake, W. Frensley, T. Moise, *Quantitative Simulation Of A Resonant-Tunneling Diode*, J-Appl-Phys, vol. 81, no. 7, pp. 3207-3213, April 1997.

[20] A. C. Seabaugh, Texas Instruments, private communication, 1997.

[21] The actual CPU time needed for a single I-V simulation depends strongly on the choice of material systems, bandstructure models, temperature scattering models, and bias points. The individual I-V characteristics presented here take about 30 minutes to compute on a single 200 MHz R10000 CPU of an SGI Origin.

Tom Cwik is supervisor of the High Performance Computing group at the Jet Propulsion Laboratory. Prior to this position he was a Member of Technical Staff in the JPL Microwave Engineering Group, arriving at JPL in 1988. His current research is focused on the application of massively parallel computation for the numerical simulation of electromagnetic systems. This includes work in scattering and light coupling in infrared devices, lenses and filters, and the development of finite element modeling software on distributed memory computers.

Tom Cwik received his BS, MS, and Ph.D. degrees in Electrical Engineering from the University of Illinois, Urbana-Champaign, in 1979, 1981, and 1986, respectively. He has worked at the Very Large Array in Socorro, NM, the National Bureau of Standards in Boulder, CO, and as a Postdoctoral Fellow at the Norwegian Institute of Technology. In 1996 he was appointed an Affiliate Professor in the Department of Electrical Engineering, University of Washington, Seattle, WA.

Gerhard Klimeck is a senior technical staff member at the NASA Jet Propulsion Laboratory. His research interest is in the quantum mechanical modeling of electron transport through nanoelectronic devices. Previously he was a member of technical staff at the Applied Research Laboratory of Raytheon (formerly known as the Central Research Lab of Texas Instruments) where he served as manager of the Nanoelectronic Modeling (NEMO) program. The tool is available to the U.S. research community; see http://www.raytheon.com/rtis/nemo/ for details. Dr. Klimeck received his Ph.D. in 1994 from Purdue University where he studied electron transport through quantum dots, resonant tunneling diodes and 2-D electron gases. His research for his German electrical engineering degree, which he obtained in 1990 from Ruhr-University Bochum, concerned the study of laser noise propagation. Dr. Klimeck's work is documented in over 40 publications. He is a member of IEEE, APS, HKN and TBP.